Accurate FDTD Dispersive Modeling for Concrete Materials

Haejun Chung, Jeahoon Cho, Sang-Gyu Ha, Saehoon Ju, and Kyung-Young Jung

This work presents an accurate finite-difference time-domain (FDTD) dispersive modeling of concrete materials with different water/cement ratios in 50 MHz to 1 GHz. A quadratic complex rational function (QCRF) is employed for dispersive modeling of the relative permittivity of concrete materials. To improve the curve fitting of the QCRF model, the Newton iterative method is applied to determine a weighting factor. Numerical examples validate the accuracy of the proposed dispersive FDTD modeling.

Keywords: FDTD, dispersive media, concrete materials, Newton iterative method.

I. Introduction

The finite-difference time-domain (FDTD) method [1]-[4] is highly suitable for the transient analysis of electromagnetic wave propagation in the existence of concrete materials in a wide range of research areas, such as wireless indoor communication systems [5], ground-penetrating radar [6], nondestructive testing [7], and high-power electromagnetics [8]. In the FDTD method, it is of great importance to accurately represent dispersive characteristics of concrete materials. Nevertheless, dispersive modeling of concrete materials has not been considered in most previous literature. So far, the extended one-pole Debye model [9], the Cole-Cole model [9], and the Jonscher model [10] have been suggested to represent frequency dependency of concrete materials. Among these dispersion models, the Cole-Cole model and the Jonscher model show agreement with the measured complex relative permittivity of concrete materials. However, dispersive FDTD modeling of these two models cannot be easily employed due to overwhelming computational burdens because fractional derivatives are involved in their equations [11]. Based on a quadratic complex rational function (QCRF), in this work, FDTD dispersive modeling suitable for concrete materials is presented. To improve the accuracy of the QCRF model, the Newton iterative method is employed to determine a weighting factor (WF) of the weight least square method (WLSM) for the QCRF model. Numerical examples illustrate the accuracy of the proposed dispersive FDTD model.

Manuscript received Nov. 6, 2012; revised Feb. 6, 2013; accepted Feb. 27, 2013.

This work was supported by the research fund of the Attached Institute of ETRI.

Haejun Chung (phone: +1 765 714 7229, pino85@naver.com) was with the Department of Electronics Computer Engineering, Hanyang University, Seoul, Rep. of Korea, and is now with the School of Electrical and Computer Engineering, Purdue University, West Lafayette, IN, USA.

Jeahoon Cho (nflog@hanyang.ac.kr), Sang-Gyu Ha (godhsk_mylover@nate.com), and Kyung-Young Jung (corresponding author, kyjung3@hanyang.ac.kr) are with the Department of Electronics Computer Engineering, Hanyang University, Seoul, Rep. of Korea.

Saehoon Ju (saehoonju@ensec.re.kr) is with the Electromagnetic Wave Research Department, Attached Institute of ETRI, Daejeon, Rep. of Korea.

http://dx.doi.org/10.4218/etrij.13.0212.0491

II. QCRF-Based Dispersive FDTD for Concrete Materials

We employ the QCRF model for the relative complex permittivity of concrete materials:

$$\varepsilon_{r,\mathrm{QCRF}}(\omega) = \frac{A_0 + A_1(j\omega) + A_2(j\omega)^2}{1 + B_1(j\omega) + B_2(j\omega)^2}, \quad (1)$$

where the A_0, A_1, A_2, B_1, and B_2 coefficients can be determined by solving a 5×5 matrix inversion without any initial values [12]. Since the permittivity of concrete materials shows rapid variations below 100 MHz, WLSM is introduced to improve the accuracy of QCRF. WLSM emphasizes the places where the significant variation of the dispersion curve occurs by giving more weights. Toward this purpose, a WF is multiplied to the matrix equation of the QCRF model. In this work, we define $WF(\omega_i) = (1/\omega_i)^{\alpha}$, for which α is optimized by the

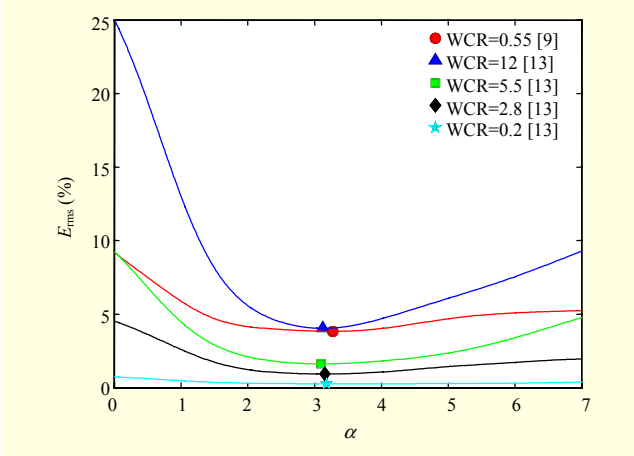

Fig. 1. Error depending on α with various WCRs. Symbols indicate minimum error.

Newton iterative method. Note that we choose $\alpha \geq 0$ because the complex relative permittivity of concrete materials varies rapidly at low frequencies. To determine the best α, the root mean square error (E_{rms}) is estimated by comparing the QCRF model with the measured relative permittivity data of concrete materials:

$$E_{rms} = \sqrt{\frac{\sum_{i}^{N} \left| \varepsilon_{r,QCRF}(\omega_i) - \varepsilon_{r,data}(\omega_i) \right|^2}{\sum_{i}^{N} \left| \varepsilon_{r,data}(\omega_i) \right|^2}}, \quad (2)$$

where $\varepsilon_{r,data}(\omega_i)$ is the measured relative permittivity from [9] and [13]. The Newton iterative method is applied to minimize this error. To validate the accuracy of the proposed method, measured data for five concrete materials, each with a different water/cement ratio (WCR), is used. The accuracy of two cases, unweighted QCRF ($\alpha = 0$) and Newton-optimized QCRF, is shown in Fig. 1. As shown in this figure, Newton-optimized QCRF always yields better results than unweighted QCRF. Table 1 summarizes the optimal α, the corresponding error, and the final QCRF coefficients. It turns out that the errors are 0.2% to 4%. Even though the 4% error seems high, it is significantly decreased from 25% by applying the proposed method. Note that the real part of the poles on the $j\omega$ plane should be negative to satisfy the Krammer-Kronig relations, that is, the causality condition [14]. This requirement is satisfied when the coefficients of the denominator (B_1 and B_2) are positive. Concrete materials are lossy, and the QCRF model thus meets this stability criterion (see Table 1).

As shown in Fig. 2, we compare the QCRF model and the measured data for the real and imaginary parts of the complex relative permittivity of concrete materials. For comparison, we also consider the extended one-pole Debye model [9]. The QCRF model agrees well with the measured data, but the extended one-pole Debye model does not fit with the measured data. It is worthy of noting that the relative permittivity of the measured data in [9] is larger than that of the measured data in

Table 1. Optimal α, corresponding error, and QCRF coefficients.

	WCR 0.55	WCR 12	WCR 5.5	WCR 2.8	WCR 0.2
α	3.2708	3.1263	3.1010	3.1577	3.1814
E_{rms}	3.828%	4.044%	1.627%	0.922%	0.268%
A_0	30.902	60.757	18.846	13.003	4.842
A_1	$6.16e^{-8}$	$1.69e^{-7}$	$9.48e^{-8}$	$1.03e^{-7}$	$1.37e^{-8}$
A_2	$9.84e^{-18}$	$3.49e^{-17}$	$2.44e^{-17}$	$2.61e^{-17}$	$3.23e^{-18}$
B_1	$4.71e^{-9}$	$1.45e^{-8}$	$1.27e^{-8}$	$1.74e^{-8}$	$2.96e^{-9}$
B_2	$1.21e^{-18}$	$4.78e^{-18}$	$4.28e^{-18}$	$5.16e^{-18}$	$7.29e^{-19}$

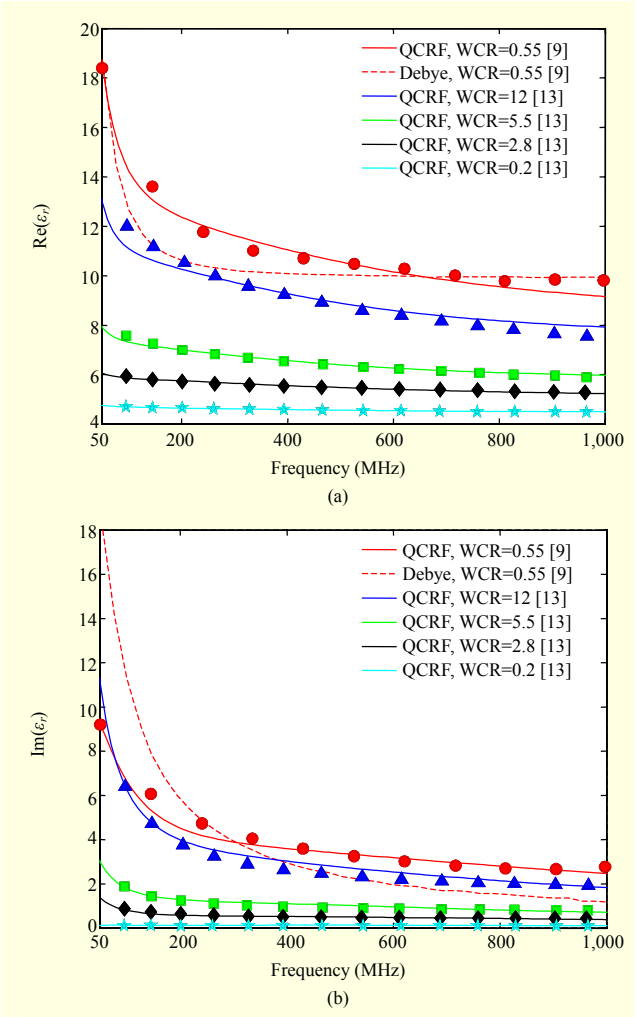

Fig. 2. Relative complex permittivity of various concrete samples. QCRF model (solid lines), extended one-pole Debye model (dashed line), and measured data (symbols). (a) Real part and (b) imaginary part.

[13], even though the WCR of the former is smaller than that of the latter. This can be explained by the fact that the relative permittivity of concrete materials depends not only on WCR but on such other factors as aggregates, porosity, and incubation time [13].

The FDTD update equations can be obtained by using the constitutive relation, that is, $\mathbf{D}(\omega)=\varepsilon_0\varepsilon_{r,\mathrm{QCRF}}(\omega)\mathbf{E}(\omega)$, and then applying the inverse Fourier transform and standard difference scheme [1]. For example, the update equation of E_x is written as

$$E_x^{n+1}=c_aE_x^n+c_bE_x^{n-1}+c_cD_x^{n+1}+c_dD_x^n+c_eD_x^{n-1}, \quad (3)$$

where $c_a=-2(a_0-a_2)/(a_1+a_2)$, $c_b=(a_1-a_2)/(a_1+a_2)$, $c_c=(b_1+b_2)/(a_1+a_2)$, $c_d=2(b_0-b_2)/(a_1+a_2)$, and $c_e=-(b_1-b_2)/(a_1+a_2)$, with $a_0=A_0\Delta t^2$, $a_1=A_1\Delta t$, $a_2=2A_2$, $b_0=\Delta t^2/\varepsilon_0$, $b_1=B_1\Delta t/\varepsilon_0$, and $b_2=2B_2/\varepsilon_0$. The update equations of E_y and E_z can be written in a simiar fashion, and the update equations of **D** and **H** can be straightfowardly obtained by employing the standard difference scheme for Maxwell's curl equations. Note that the computational costs (computational time and memory requirement) of the QCRF-based FDTD are significantly less than those of other dispsersive FDTD models involving fractional derivatives [11], such as the Cole-Cole model and the Jonscher model.

III. Numerical Examples

To validate the accuracy of the proposed dispersive FDTD, both theoretical results and nondispersive FDTD results are used for the concrete sample presented in [9]. First, the accuracy of QCRF-based dispersive FDTD is verified against theory. In a 1D simulation, a uniform plane wave is incident from air to the concrete region at z=0. The reflection coefficient (Γ) and the transmission coefficient (τ) are calculated at z=0. For the theoretical values, $\Gamma=(\eta_1-\eta_0)/(\eta_1+\eta_0)$ and $\tau=2\eta_1/(\eta_1+\eta_0)$ are calculated, where $\eta_0=\sqrt{\mu_0/\varepsilon_0}$ and $\eta_1=\sqrt{\mu_0/\varepsilon_0\varepsilon_{r,\mathrm{data}}(\omega)}$. As shown in Fig. 3, both coefficients from the QCRF-based dispersive FDTD agree very well with those of the theoretical approach.

In addition, the QCRF-based dispersive FDTD is compared with the nondispersive FDTD. The simulation is performed on a 2D space (100 × 100 cells), and a square-shaped concrete region (20 × 20 cells) is located at the center of the simulation region. The source point is located 30 cells away from the center of the concrete region. Four different cases (Δs = 0.2 mm, 1 mm, 5 mm, and 10 mm) are considered in this simulation, where Δs indicates the FDTD grid size. Note that the largest FDTD grid size is approximately 1/10 of wavelength at the maximum frequency (1 GHz). We calculate

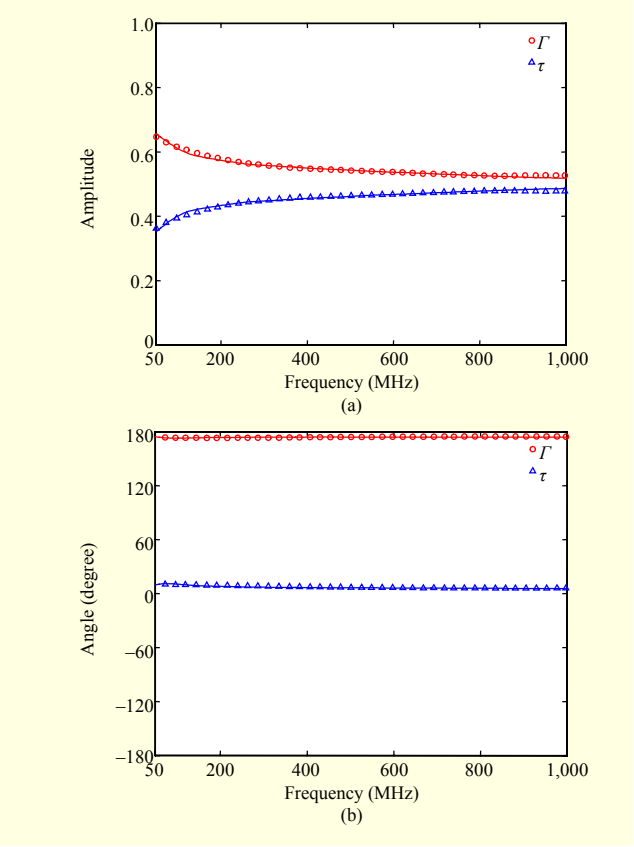

Fig. 3. Reflection and transmission coefficients of concrete sample. Solid lines and symbols represent QCRF-based dispersive FDTD and theory, respectively. (a) Amplitude of reflection and transmission coefficients and (b) angle of reflection and transmission coefficients.

the propagation loss at the center of the concrete region (Loss 1) and at the outside of the concrete region, 30 cells away from the center (Loss 2). In the nondispersive FDTD simulation, a DC-offset sine wave [15] is excited and many simulations are performed over the frequency of interests. In this simulation, conventional FDTD update equations for lossy dielectrics [1], [8] are used and the values of relative permittivity and conductivity are used from the measured data [9]. Note that only one simulation is performed under a differential-Gaussian-modulated sine wave excitation for the QCRF-based dispersive FDTD, and the frequency response can be obtained by the discrete Fourier transform [16]. As illustrated in Fig. 4, both simulations show agreement. Note that the physical sizes of the concrete region are different for four cases, and different spectral behaviors for the propagation loss are thus observed.

IV. Conclusion

We developed QCRF-based FDTD dispersive algorithms

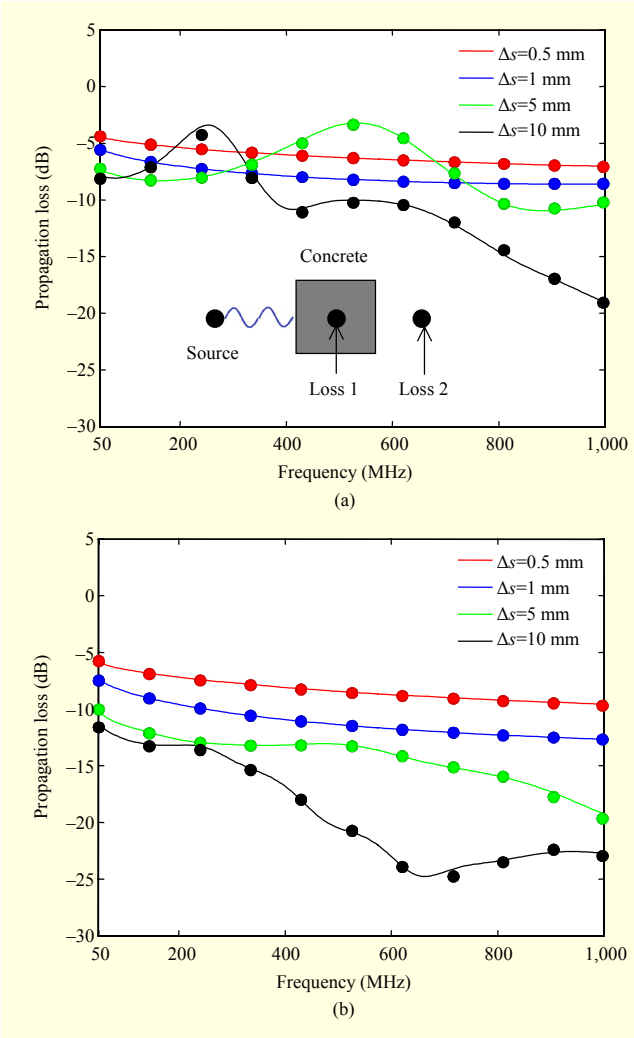

Fig. 4. Propagation loss. Solid lines and symbols represent QCRF-based dispersive FDTD and non-dispersive FDTD, respectively. (a) Loss 1 and (b) Loss 2.

suitable for the analysis of concrete materials in 50 MHz to 1 GHz. The Newton iterative method was applied to improve the accuracy of dispersive modeling of concrete materials. The accuracy of the proposed dispersive FDTD for concrete materials was verified through numerical examples. Although the proposed QCRF-based FDTD dispersive modeling of concrete materials was presented for the frequency range of 50 MHz to 1 GHz, it can be straightforwardly extended to other frequency ranges whenever the measured relative permittivity data of concrete materials are available.

References

[1] A. Taflove and S.C. Hagness, *Computational Electrodynamics: The Finite-Difference Time-Domain Method*, 3rd ed., Artech House, 2005.

[2] K.-Y. Jung, F.L. Teixeira, and R.M. Reano, "Au/SiO_2 Nanoring Plasmon Waveguides at Optical Communication Band," *J. Lightw. Technol.*, vol. 25, no. 9, 2007, pp. 2757-2765.

[3] X. Duan et al., "Analysis on the Calculation of Plasma Medium with Parallel SO-FDTD Method," *ETRI J.*, vol. 31, no. 4, Aug. 2009, pp. 387-392.

[4] K.-P. Hwang, "A fourth-order accurate numerical boundary scheme for the planar dielectric interface: a 2-D TM case," *J. Electromag. Eng. Sci.*, vol. 11, no. 1, 2011, pp. 11-15.

[5] A.C.M. Austin, M.J. Neve, and G.B. Bowe, "Modeling Propagation in Multifloor Buildings Using the FDTD Method," *IEEE Trans. Antennas Propag.*, vol. 59, no. 11, 2011, pp. 4239-4246.

[6] G. Klysz, J.P. Balayssac, and X. Ferrieres, "Evaluation of Dielectric Properties of Concrete by a Numerical FDTD Model of a GPR Coupled Antenna-Parametric Study," *NDT&E Int.*, vol. 41, 2008, pp. 621-631.

[7] O. Gunes and O. Buyukozturk, "Simulation-Based Microwave Imaging of Plain and Reinforced Concrete for Nondestructive Evaluation," *Int. J. Phys. Sci.*, vol. 7, no. 3, 2012, pp. 383-393.

[8] C. Bin et al., "Analysis of Shielding Effectiveness of Reinforced-Concrete in High Power Electromagnetic Environment," *APCEEM*, 2003, pp. 547-553.

[9] A. Robert, "Dielectric Permittivity of Concrete between 50 MHz and 1 GHz and GPR Measurements for Building Materials Evaluation," *J. Appl. Geophys.*, vol. 40, 1998, pp. 89-94.

[10] T. Bourdi et al., "Application of Jonscher Model for the Characterization of the Dielectric Permittivity of Concrete," *J. Phys. D*, vol. 41, 2008, pp. 205410:1-205410:9.

[11] F. Torres, P. Vaudon, and B. Jecko, "Application of Fractional Derivatives to the FDTD Modeling of Pulse Propagation in Cole-Cole Dispersive Medium," *Microw. Opt. Technol. Lett.*, vol. 13, no. 5, 1996, pp. 300-304.

[12] E.C. Levi, "Complex-Curve Fitting," *IRE Trans. Autom. Control*, vol. 4, 1959, pp. 37-44.

[13] M.N. Soutsos et al., "Dielectric Properties of Concrete and Their Influence on Radar Testing," *NDT&E Int.*, vol. 34, 2001, pp. 419-425.

[14] F.L. Teixeira and W.C. Chew, "On Causality and Dynamic Stability of Perfectly Matched Layers for FDTD Simulations," *IEEE Trans. Microw. Theory Tech.*, vol. 47, no. 6, 1999, pp. 775-785.

[15] C.M. Furse et al., "The Problem and Treatment of DC Offsets in FDTD Simulations," *IEEE Trans. Antennas Propag.*, vol. 48, no. 8, 2000, pp. 1198-1201.

[16] C.M. Furse and O.P. Gandhi, "Why the DFT is Faster Than the FFT for FDTD Time-to-Frequency Domain Conversion," *IEEE Microw. Guided Wave Lett.*, vol. 5, no. 10, 1995, pp. 326-328.